Korean J. Chem. Eng., **27**(4), 1310-1315 (2010)
DOI: 10.1007/s11814-010-0182-y

Characterization and synthesis of Ce-incorporated mesoporous molecular sieves under microwave irradiation condition

Qian Zhao*,,†, Qian Wang*, Yajing Tang*, Tingshun Jiang*, Chang-sheng Li**, and Hengbo Yin***

*School of Chemistry and Chemical Engineering, **School of Material Science & Engineering,
Jiangsu University, Xuefu Road 301#, Zhenjiang 212013, P. R. China
(*Received 22 July 2009 • accepted 16 November 2009*)

Abstract−Ce-incorporated MCM-41 mesoporous molecular sieves (CeMCM-41) were synthesized by microwave irradiation method from sodium silicate and ammonium cerium (IV) nitrate precursors and using cetyltrimethyl ammonium bromide (CTAB) as template. The resulting samples were characterized by means of XRD, TEM, FT-IR, UV-Vis, XPS and N_2 physical adsorption, respectively. The effect of the Si/Ce molar ratio on the textural properties of CeMCM-41 was investigated. The results reveal that the CeMCM-41 was successfully synthesized. The resultant mesoporous materials have specific surface areas in the range of 602-1,216 m^2/g and pore sizes in the range of ca. 2.6-2.9 nm. The structural properties are related to the amount of cerium incorporation. The surface area and pore volume of the resulting CeMCM-41 were gradually reduced as the cerium content in the sample increased, and the mesoporous ordering diminished.

Key words: Ce-incorporated Mesoporous Molecular Sieve, Microwave Irradiation Method, Synthesis, Characterization, Textural Property

INTRODUCTION

Since the initial report of a new family of mesoporous molecular sieves named as M41S by Mobil Company in the early 1900s [1], a vital breakthrough in the field of the porous materials took place. Since then, the synthesis of mesoporous materials has aroused considerable interest among worldwide researchers. The increased interest is based on the presence of a well-defined ordered mesoporous structure which provides outstanding textural characteristics such as uniform pore size and high specific surface area for the new material. In the M41S family, MCM-41 mesoporous molecular sieve is probably the most widely investigated due to its hexagonal array of uniform mesopores with uniform pore size ranging from 2 to 10 nm. Over the last decades, it has been found that the MCM-41 mesoporous molecular sieve has some potential application in the fields of adsorption, catalysis, fine chemical industries, synthesis of the nanometer cluster, medicine and environmental protection [2-9]. Unfortunately, the pure silica-based MCM-41 mesoporous molecular sieve exhibits low catalytic activity, weak surface acidity and poor stability, which limits its application in many acid-catalyzed reactions. This bottleneck has not been overcome completely. Recently, in order to obtain better catalytic performance and to improve its potential application in many fields, various transition metals such as Al, Mo, Cu, Co, V, Fe, Nd, Ce, Ni [3,5,10-13] have been incorporated into the framework of MCM-41 mesoporous molecular sieve and the resultant mesoporous materials have had remarkable catalytic performance [3,10,11]. Nowadays, cerium-containing materials have attracted much attention due to their potential application in various kinds of reactions [14-16]. Among these materials, cerium-incorporated MCM-41 mesoporous molecular sieve is particularly of interest because of the important application in catalytic reactions [17,18]. However, most of the previous reports focused on the hydrothermal synthesis of Ce-containing mesoporous molecular sieve and the investigation of the catalytic property. The hydrothermal synthesis process requires a long crystallization time and high crystallization temperature. Compared with the hydrothermal method, microwave irradiation technique has some advantages such as microwave dielectric heating, short crystallization time, ease of carrying out, and environmental friendliness. By far, the synthesis of CeMCM-41 mesoporous molecular sieve through microwave irradiation methods was seldom reported.

For this purpose, in the current work, Ce-incorporated MCM-41 mesoporous molecular sieves were synthesized by microwave irradiation method. And an investigation on the effect of the different molar ratio of Si/Ce on the mesoporous ordering and the textural property (the specific surface areas and pore volume) of the resulting CeMCM-41 mesoporous materials was also carried out. At the same time, the resultant materials were characterized by various physicochemical methods, including XRD, TEM, FT-IR, UV-vis, XPS and N_2 physical adsorption.

EXPERIMENTAL

1. Chemicals

Sodium silicate ($Na_2SiO_3 \cdot 9H_2O$), ammonium cerium nitrate ($Ce(NH_4)_2(NO_3)_6$), cetyltrimethyl ammonium bromide (CTAB), and concentrated sulfuric acid (H_2SO_4), were purchased from Shanghai Chemical Reagent Corporation, China. All reagents were of analytical grade.

2. Synthesis of Ce-incorporated MCM-41 Mesoporous Molecular Sieve under Microwave Irradiation Condition

The synthesis of Ce-incorporated mesoporous molecular sieve was carried out by the microwave irradiation method. The molar

†To whom correspondence should be addressed.
E-mail: qianzhao@ujs.edu.cn

Table 1. Analysis results of surface areas, average pore sizes, pore volumes and XRD of the samples

Sample	$(Si/Ce)^a_{gel}$	$(Si/Ce)_{solid}$	Surface area/(m^2g^{-1})	Average pore size/nm	Pore volume/(cm^3g^{-1})	d^b_{100}/nm	a^c_0/nm
MCeMCM-41(1)	99	100	1216	2.6	0.98	3.9	4.5
MCeMCM-41(2)	49	51	859	2.7	0.88	4.1	4.7
MCeMCM-41(3)	24	25	602	2.9	0.65	-	-

[a]Si/Ce molar ratio in gel; [b]$d_{100}=\lambda/2\sin\theta$; [c]$a_0=2d_{100}/\sqrt{3}$

ratio of Si: CTAB: Ce: H_2O in the starting materials was (1-x): 0.25: x: 100 (x=0.01, 0.02, 0.04, respectively). A brief description of the synthesis procedure was as follows: First, a given amount of Ce $(NH_4)_2(NO_3)_6$ was dispersed in 30 ml distilled water, a given amount of $Na_2SiO_3\cdot 9H_2O$ was dissolved in 100 ml distilled water, and 9.11 g of CTAB was dispersed in 50 ml distilled water until a gelatinous solution was obtained, and then sodium silicate ($Na_2SiO_3\cdot 9H_2O$) solution was added into ammonium cerium nitrate solution under stirring. The resulting mixture was slowly added into the gelatinous solution under vigorous stirring for 10 min and the pH value of the mixed solution was adjusted to 11 by dropwise addition of sulfuric acid (5 mol/*l*). After stirring for 80 min, the resulting suspension was transferred into a 250 ml round-bottomed quartz flask, and then the round-bottomed quartz flask was placed into a microwave oven with a refluxing condenser and heated at boiling point for 2.5 h under continuous microwave irradiation with a power of 220 W (National NN-S570MFS). After cooling to room temperature, the sample was filtered, washed with deionized water, and dried at 100 °C for 24 h. As a result, a dried sample was obtained, denoted as s-MCeMCM-41(X), where X stands for the sample number from 1 to 3, according to cerium content added in the synthesis procedure. The s-MCeMCM-41(X) sample was heated to 550 °C at a heating rate of 2 °C/min and calcined at 550 °C in air for 10 h, and the calcined sample was named as MCeMCM-41(X). The Si content in the samples determined by gravimetric method and Ce content in the samples determined by the inductive coupled plasma (ICP) technique are summarized in Table 1.

For comparison, the pure silica MCM-41 mesoporous molecular sieve was synthesized under exactly the same conditions as the MCeMCM-41 mesoporous molecular sieve except that the ammonium cerium nitrate was not added in the starting material. The dried sample was designated as s-MCM-41, and the calcined sample was denoted as MCM-41. At the same time, Ce-loaded MCM-41 mesoporous molecular sieve was prepared by wet impregnation method using 10% ammonium cerium nitrate solution, and the obtained sample was designated as Ce/MCM-41. The Ce content loaded on the sample MCM-41 is consistent with the sample MCeMCM-41(2).

3. Characterization

The X-ray diffraction (XRD) patterns of samples were recorded with a powder XRD instrument (Rigaku D/max 2500PC) with Cu K_α radiation (λ=0.154 18 nm). It was operated at 40 kV and 50 mA. The experimental conditions correspond to a step width of 0.02° and the scan speed of 1°/min. The diffraction patterns were recorded in the 2θ range of 1-10°. Fourier transform infrared spectra of samples were recorded on a Nexus FT-IR 470 spectrometer made by Nicolet Corporation (USA) with KBr pellet technique. The effective range was from 400 to 4,000 cm^{-1}. Specific surface area and pore size were measured by using a NOVA2000e analytical system made by Quantachrome Corporation (USA). The specific surface area was calculated by Brunauer-Emmett-Teller (BET) method. Pore size distribution and pore volume were calculated by Barrett-Joyner-Halenda (BJH) method. Transmission electron microscopy (TEM) morphologies of samples were observed on a Philips TEMC-NAI-12 with an acceleration voltage of 100-120 kV. Diffuse reflectance UV-Vis spectra were recorded on a UV-3100 spectrophotometer made by Shimadzu Corporation (Japan) with spherical diffuse reflectance accessory, using $BaSO_4$ as a reference. The cerium content in the samples was determined by inductively coupled plasma (ICP) technique (Vista-MAX, Varian). X-ray photoelectron spectroscopy (XPS) analysis was carried out on an ESCALAB 250 (Thermal Electron Corp.) spectrometer equipped with Al Kα X-ray source, operating at 150 W. The binding energies were referenced to the C1s binding energy at 284.8 eV.

RESULTS AND DISCUSSION

1. XRD Analysis

The low-angle powder X-ray diffraction patterns of the samples CeMCM-41 are shown in Fig. 1. It can be observed that the two samples MCeMCM-41(1) and MCeMCM-41(2) have a diffraction peak (100) at 2θ value of ca. 2.2°, respectively. This clearly indicates that the CeMCM-41 samples synthesized by microwave irradiation method possess mesoporous framework and small amount of cerium ions incorporated into the framework of the MCM-41 mesoporous molecular sieve does not significantly modify the crystalline structure of the resultant materials. However, compared with the pattern of the typical MCM-41 mesoporous molecular sieve

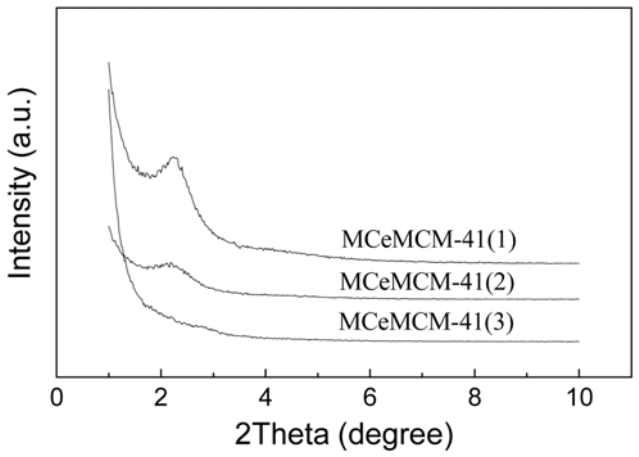

Fig. 1. XRD patterns of the samples CeMCM-41 synthesized by microwave irradiation according to the different molar ratio of Si/Ce after calcination at 550 °C for 10 h.

[1], it can be noted that the diffraction peaks (110, 200 and 210) of the resulting samples disappeared after Ce ions were incorporated into the framework of the pure silica MCM-41 mesoporous molecular sieve and the intensity of the peak (100) also decreased, indicating that the cerium ions were incorporated into the framework of MCM-41 and the long range ordering of the resulting mesoporous materials deteriorated. It is postulated that the confusion of the mesoporous framework was due to the change of Si-O-Si bond angle aroused by cerium ions incorporated into the silica-based framework of MCM-41, resulting in the deterioration of the crystallinity of the MCM-41 mesoporous molecular sieve. According to Ref. [19], the CeMCM-41 sample synthesized via microwave irradiation method only has a diffraction peak (100), but it still possesses the short range and hexagonal arrangement mesoporous structure. Additionally, as shown in Fig. 1, with the increase of the Ce content in the sample, the diffraction peak (100) of the sample CeMCM-41 was broad and weak, and intensity of the diffraction peak (100) also decreased. At the same time, we can also observe that the diffraction peak (100) of the sample MCeMCM-41(3) disappeared, but combined with the surface area data (602 m^2/g) listed in Table 1, the MCeMCM-41(3) still has the partial mesoporous framework. However, the mesoporous ordering is poor. This is probably attributed to Si^{4+} in the pure silica MCM-41 framework is overfull substituted by Ce ions resulting in the deterioration of the symmetry of MCM-41 mesoporous molecular sieve.

2. TEM Analysis

The TEM images of the samples MCeMCM-41(1) and MCeMCM-41(2) are shown in Fig. 2. It is observed that the two samples exhibited the hexagonal arrays structure, indicating that the two samples synthesized under microwave irradiation condition possess the mesoporous framework. However, the mesoporous ordering of the sample MCeMCM-41(2) is poor as compared with that of the sample MCeMCM-41(1). Additionally, it can also be observed that there are not the particles and/or clusters containing cerium species on the surface of the two samples in Fig. 2. Generally, if the particles (or clusters) cannot be observed on the external surface of the sample illustrated in the TEM image, it is postulated that the particles (or clusters) have been incorporated into the framework of the MCM-41 mesoporous molecular sieve [20].

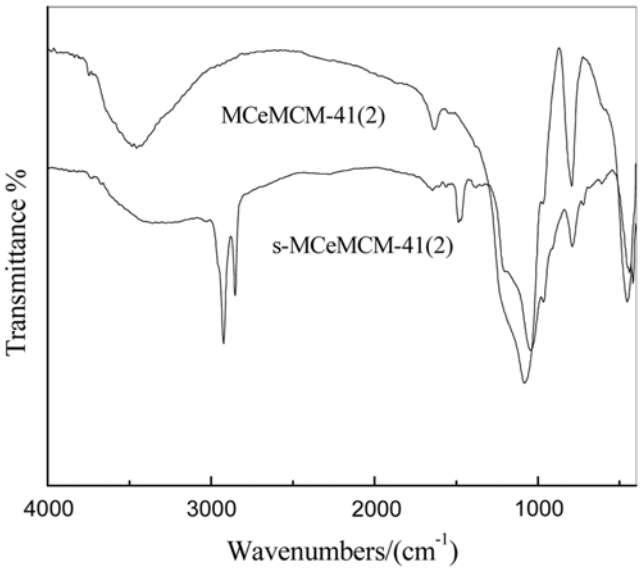

Fig. 3. FT-IR spectra of the sample MCeMCM-41(2) synthesized according to the molar ratio of 49 (Si/Ce) before and after calcination at 550 °C for 10 h.

3. FT-IR Analysis

Fig. 3 presents the FT-IR spectra of the synthesized MCeMCM-41(2) sample before and after calcination at 550 °C for 10 h. As shown in Fig. 3, the band at 3,500 cm^{-1} is the characteristic band of the water adsorbed on the sample surface. The bands at 1,620-1,640 cm^{-1} are aroused by the flexion vibration of the OH bond [21]. The band at 1,080 cm^{-1} is from the asymmetric extension vibration of Si-O-Si; The band about 810 cm^{-1} is due to the corresponding symmetric vibration of Si-O-Si bond, while the band at 460 cm^{-1} is assigned to rocking vibration of the Si-O-Si bond. The bands at 2,921, 2,850 and 1,480 cm^{-1} are the characteristic bands of the surfactant alkyl chains. After the sample MCeMCM-41(2) was calcined at

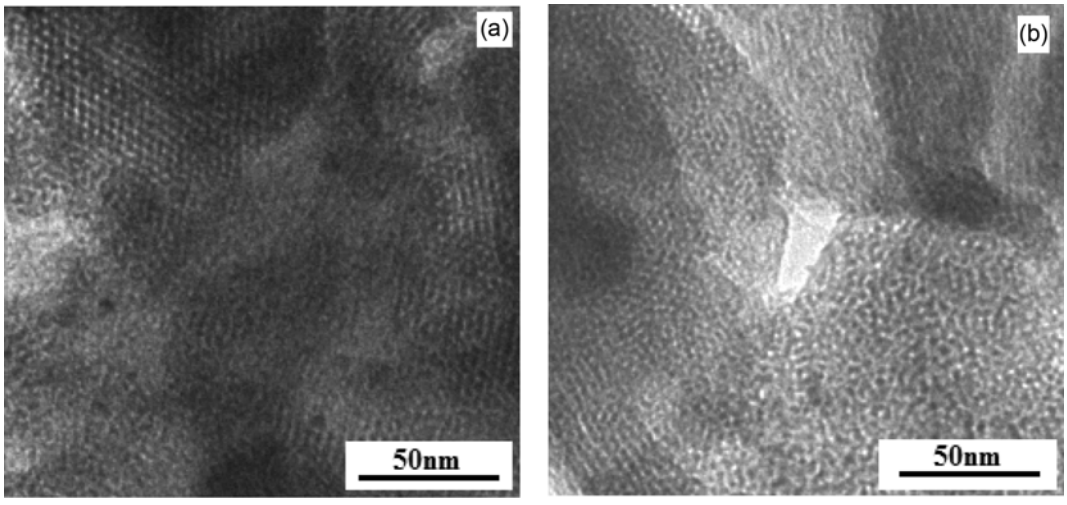

Fig. 2. TEM images of the samples MCeMCM-41(1) and MCeMCM-41(2) after calcination at 550 °C for 10 h.
(a) MCeMCM-41(1); (b) MCeMCM-41(2)

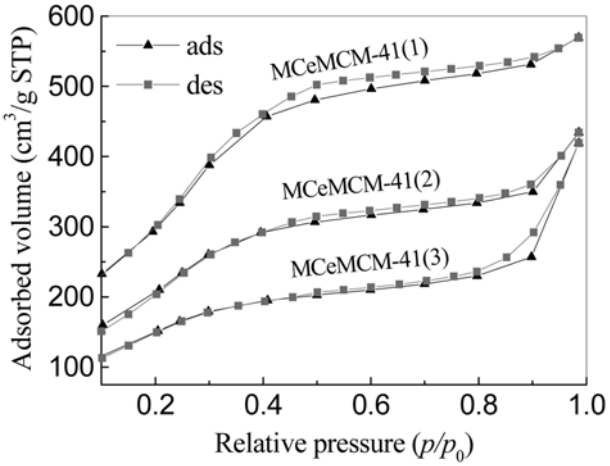

Fig. 4. N_2 physical adsorption-desorption isotherms of the samples MCeMCM-41 synthesized according to the different molar ratio of Si/Ce after calcination at 550 °C for 10 h.

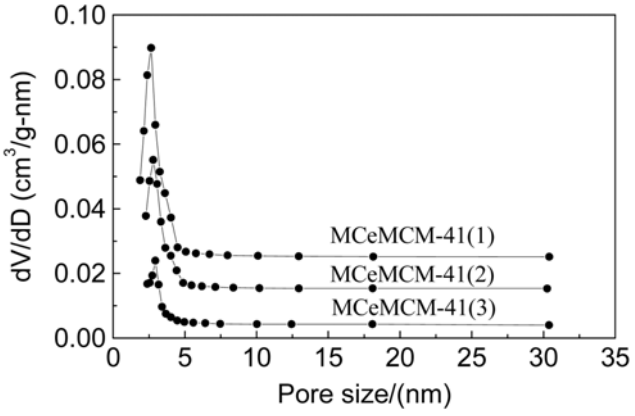

Fig. 5. Pore size distribution curves of the samples CeMCM-41 synthesized according to the different molar ratio of Si/Ce after calcination at 550 °C for 10 h.

550 °C for 10 h, the bands at 2,921, 2,850 and 1,480 cm^{-1} disappeared, certifying that the template had been effectively removed.

4. Results of Nitrogen Physical Adsorption

The porosity of the samples was evaluated by N_2 adsorption isotherms. Fig. 4 shows the N_2 adsorption-desorption isotherms of the three samples CeMCM-41 after calcination at 550 °C for 10 h. The specific surface areas and pore size distributions and pore volumes calculated by BET and BJH methods are summarized in Table 1. According to Fig. 4, the N_2 adsorption-desorption isotherms of the two samples (MCeMCM-41(1) and MCeMCM-41(2)) exhibit typical type IV isotherms with hysteresis loop caused by capillary condensation in mesopores, manifesting that the two samples possess the obvious mesoporous structure [1]. There are three well-defined stages in the isotherms of the two samples that may be identified: the isotherms show a step at the relative pressure (p/p_0) of ca. 0.3-0.4, characteristic of capillary condensation of uniform mesoporous materials, showing that the two samples have uniform pore size distribution and larger pore volume. The isotherms corresponding to $p/p_0<0.3$ are due to a monolayer adsorption of nitrogen on the walls of the mesopore. The near horizontal section beyond $p/p_0>0.4$ represents the multilayer adsorption on the outer surface of the particles. In addition, from Fig. 4, we can observe that the isotherms of the sample MCeMCM-41 (1) have a sharper capillary condensation step at the same p/p_0, illustrating that it possesses more uniform pore size distribution as compared with the isotherms of other sample. Moreover, the isotherms of the sample MCeMCM-41 (3) did not belong to a typical type IV isotherms; this is attributed to the damage of the mesoporous structure caused by the overfull cerium ions incorporated into the MCM-41 mesoporous molecular sieve. However, combined with the surface area data (602 m^2/g) listed in Table 1, the sample MCeMCM-41 (3) still has a partial mesoporous structure, but the ordering is poor.

Fig. 5 presents the pore size distribution curves of the three samples CeMCM-41 synthesized by microwave irradiation method after calcination at 550 °C for 10 h. As shown in Fig. 5, narrow and sharp peaks can be observed in an pore size range of *ca.* 2-3 nm for the samples MCeMCM-41(1) and MCeMCM-41(2), and the intensity of the peak also is strong as compared with that of the sample MCeMCM-41(3), indicating that the two samples have uniform pore size distribution as well as. Additionally, as the cerium content in the sample increased, the intensity of the pore size distribution peak became weak, which reflects that the increase of cerium ions incorporated into the silica framework of MCM-41 mesoporous molecular sieve caused the distortion of the mesoporous framework, resulting in the uneven pore size distribution and the poor mesoporous ordering.

From Table 1, we can conclude that the specific surface area and pore volume of the resulting samples gradually decreased as the cerium content increased, and the pore size is in the range of 2.6-2.9 nm. Combined with the results of XRD and N_2 adsorption isotherms, it is reasonable to conclude that the mesoporous ordering of the sample CeMCM-41 synthesized by microwave irradiation method gradually decreased with the increase of the cerium content incorporated into the mesoporous framework.

5. Diffuse Reflectance UV-vis Spectroscopy

The diffuse reflectance UV-vis spectra of the three samples CeMCM-41 are presented in Fig. 6. As shown in Fig. 6, it can be

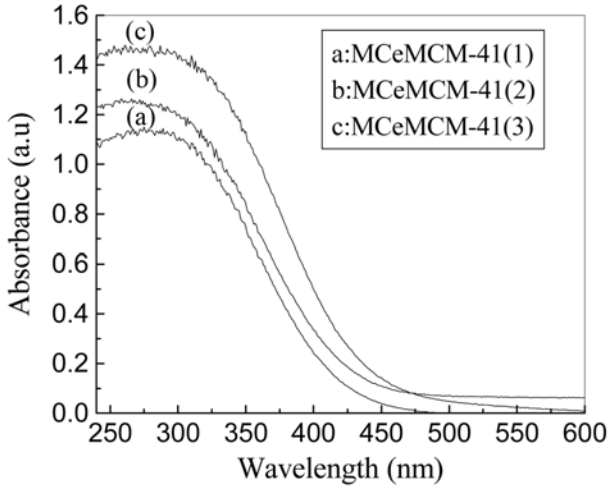

Fig. 6. Diffuse reflectance UV-vis spectra of the samples CeMCM-41 synthesized according to the different molar ratio of Si/Ce after calcination at 550 °C for 10 h.

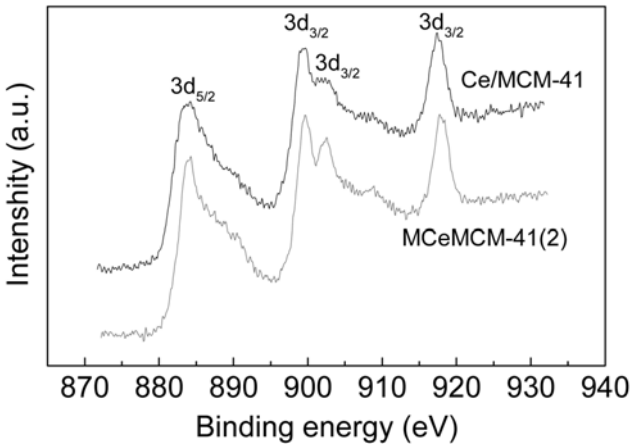

Fig. 7. Ce 3d XPS spectra of the samples Ce/MCM-41 and MCeMCM-41(2).

observed that the samples MCeMCM-41 all show one single peak with maximum at ca. 290 nm and the intensity also increases with the increase in the Ce content of the samples, which agrees with the results from the Ref. [22]. Generally, the position of the adsorption peak associated with ligand to metal charge transfer ($O^{2-} \rightarrow Ce^{4+}$) spectra depends on the ligand field symmetry surrounding the cerium center. And the electronic transitions from oxygen to tetra-coordinated Ce^{4+} require a higher energy as compared with hexa-coordinated one. Therefore, it may be suggested that the adsorption peak at ca. 290 nm for the samples CeMCM-41 is probably attributed to the presence of one type of cerium species-tetra-coordinated Ce^{4+}. It is postulated that the Ce (IV) species has been incorporated into the framework of the sample MCM-41 [17,22,23].

6. XPS Analysis

Fig. 7 displays the XPS spectra of the Ce 3d of the samples Ce/MCM-41 and MCeMCM-41(2). As shown in Fig. 7, the peak located at 883.3 eV can be assigned to the Ce $3d_{5/2}$ peak of the sample Ce/MCM-41. While the three peaks located at 899.1, 902.3 and 917.3 eV can be designated as the Ce $3d_{3/2}$ peak of the Ce/MCM-41 [24, 25]. At the same time, we can also observe that the Ce $3d_{5/2}$ peak of the sample MCeMCM-41 (2) is located at 883.9 eV, and the Ce $3d_{3/2}$ peaks of the sample MCeMCM-41(2) are located at 899.8, 902.6 and 917.7 eV, respectively. Compared with the sample Ce/MCM-41, the Ce 3d peaks of the sample MCeMCM-41(2) shifted to high binding energies, suggesting that the changes of the binding energies are aroused by the incorporation of Ce in the pore wall of mesoporous molecular sieve.

The XPS spectra of the O1s bonding energy in the samples Ce/MCM-41 and MCeMCM-41(2) are shown in Fig. 8(a) and (b). The O 1s peaks were deconvoluted. As presented in Fig. 8(a), for the sample Ce/MCM-41, two peaks appear in the O1s XPS spectra. The weak peak located at about 530.4 eV can be attributed to the oxygen in Ce-O linkages [26]. The intense peak at *ca.* 532.4 eV can be assigned to the Si-O bond. The oxygen atomic ratio of the two peaks is 0.32. For the sample MCeMCM-41(2), it is noticed that the weak peak at 530.6 eV is aroused by the Ce-O linkages, while the intense peak located at 533.1 eV is attributed to the Si-O bond (Fig. 8(b)). The oxygen atomic ratio of the two peaks is 0.12. The oxygen atomic ratio of the sample MCeMCM-41(2) is smaller

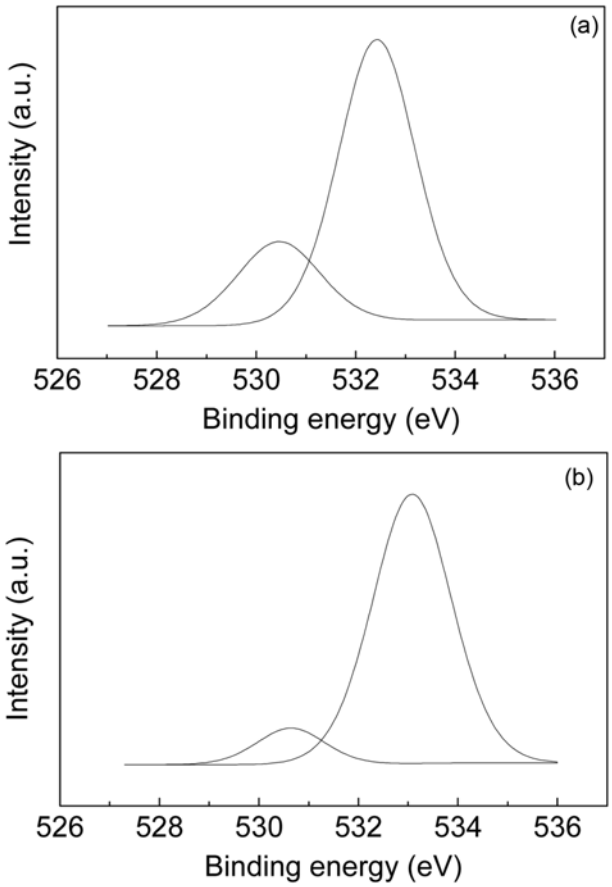

Fig. 8. O 1s XPS spectra of the samples Ce/MCM-41 and MCeMCM-41(2). (a) Ce/MCM-41; (b) MCeMCM-41(2).

than that of the sample Ce/MCM-41. Furthermore, the O1s peaks of the sample MCeMCM-41(2) shift to high binding energies as compared to the sample Ce/MCM-41. Therefore, it is reasonable to suggest that the cerium cations in the sample MCeMCM-41(2) are incorporated into the pore wall of the mesoporous molecular sieve resulting in the formation of the Ce-O-Si bond.

CONCLUSIONS

Ordered hexagonal CeMCM-41 mesoporous molecular sieves with high specific surface area were successfully synthesized via microwave irradiation method. After the synthesized sample was calcined at 550 °C for 10 h, the template was effectively removed. The Si/Ce molar ratio is a key factor influencing the textural properties and structural regularity of CeMCM-41 mesoporous molecular sieves. High cerium content is unfavorable to the formation of the CeMCM-41 with highly ordered mesoporous structure. Incorporation of cerium ions into the framework of MCM-41 mesoporous molecular sieve results in the reduction of the specific surface area and pore volume, and the mesoporous ordering deteriorated. On the other hand, the specific surface area and pore volume of the CeMCM-41 mesoporous molecular sieve decreased as the cerium content increased, and the mesoporous ordering deteriorated. In particular, the microwave irradiation method is easy to carry out; it produces even heat and is environmentally friendly.

ACKNOWLEDGEMENTS

The authors are grateful to Professor Kangmin Chen for his kind help in characterizing the samples with TEM and Mr. Junjie Jing for providing UV-vis analysis, the Test Centre of Physics and Chemistry, Jiangsu University, China.

REFERENCES

1. J. S. Beck, J. C. Vartuli, W. J. Roth, M. E. Leonowicz, C. T. Kresge, K. D. Schmitt, C. T.-W. Chu, D. H. Olson, E. W. Sheppard, S. B. McCullen, J. B. Higgins and J. L. Schlenker, *J. Am. Chem. Soc*., **114**, 10834 (1992).
2. N. Aoyama, T. Yoshihara, S. I. Furukawa, T. Nitta, H. Takahashi and M. Nakano, *Fluid Phase Equilib*, **257**, 212 (2007).
3. S. Velu, L. Wang, M. Okazaki, K. Suzuki and S. Tomura, *Microporous Mesoporous Mater*., **54**, 113 (2002).
4. T. S. Jiang, L. D. Lu, X. J. Yang and Q. Zhao, *J. Porous Mater*., **15**, 67 (2008).
5. R. Wojcieszak, S. Monteverdi, M. Mercy, I. Nowak, M. Ziolek and M. M. Bettahar, *Appl. Catal. A*, **268**, 241 (2004).
6. M. C. Kerby, T. F. Degnan Jr., D. O. Marler and J. S. Beck, *Catal. Today*, **104**, 55 (2005).
7. G. E. Mary and J. B. Kennet, *Microporous Mesoporous Mater*., **28**, 113 (1999).
8. Q. Tang, Y. Xu, D. Wu, Y. Sun, J. Wang, J. Xu and F. Deng, *J. Controlled Release*, **114**, 41 (2006).
9. S. Chaliha and K. G. Bhattacharyya, *J. Hazard. Mater*., **150**, 728 (2008).
10. S. Li, Q. Xu, J. Chen and Y. Guo, *Ind. Eng. Chem. Res*., **47**, 8211 (2008).
11. L. F. Chen, X. L. Zhou, L. E. Noreña, J. A. Wang, J. Navarrete, P. Salas, A. Montoya, P. Del Angel and M. E. Llanos, *Appl. Surf. Sci*., **253**, 2443 (2006).
12. T. S. Jiang, Q. Zhao, K. M. Chen, Y. J. Tang, L. B. Yu and H. B. Yin, *Appl. Surf. Sci*., **254**, 2575 (2008).
13. J. Xu, W. Chu and S. Luo, *J. Mol. Catal. A*, **256**, 48 (2006).
14. M. N. Timofeeva, S. H. Jhung, Y. K. Hwang, D. K. Kim, V. N. Panchenko, M. S. Melgunov, Y. A. Chesalov and J. S. Chang, *Appl. Catal. A*, **317**, 1 (2007).
15. K. M. N. Khalil, *J. Colloid Interface Sci*., **307**, 172 (2007).
16. C. Lu, W. L. Worrell, R. J. Gorte and J. M. Vohs, *J. Electrochem. Soc*., **150**, A 354 (2003).
17. M. D. Kadgaonkar, S. C. Laha, R. K. Pandey, P. Kumar, S. P. Mirajkar and R. Kumar, *Catal. Today*, **97**, 225 (2004).
18. A. S. Araujo, J. M. F. B. Aquino, M. J. B. Souza and A. O. S. Silva, *J. Solid State Chem*., **171**, 371 (2003).
19. P. T. Tanev, M. Chibwe and T. J. Pinnavaia, *Nature*, **368**, 321 (1994).
20. Q. Dai, X. Wang, G. Chen, Y. Zheng and G. Lu, *Microporous Mesoporous Mater*., **100**, 268 (2007).
21. L. F. Chen, L. E. Noreña, J. Navarrete and J. A. Wang, *Mater. Chem. Phys*., **97**, 236 (2006).
22. S. C. Laha, P. Mukherjee, S. R. Sainkar and R. Kumar, *J. Catal*., **207**, 213 (2002).
23. W. Yao, Y. Chen, L. Min, H. Fang, Z. Yan, H. Wang and J. Wang, *J. Mol. Catal. A*, **246**, 162 (2006).
24. Q. F. Chen, D. Jiang, W. M. Shi, D. Wu and Y. Xu, *Appl. Surf. Sci*., **255**, 7918 (2009).
25. B. M. Reddy, A. Khan, Y. Yamada, T. Kobayashi, S. Loridant and J. C. Volta, *J. Phys. Chem*., **106**, 10964 (2002).
26. A. Bensalem, F. Bozon-Verduraz, M. Delamar and G. Bugli, *Appl. Catal. A*, **121**, 81 (1995).